Analytica Chimica Acta 769 (2013) 114–120

Contents lists available at SciVerse ScienceDirect

Analytica Chimica Acta

journal homepage: www.elsevier.com/locate/aca

Preparation and application of triangular silver nanoplates/chitosan composite in surface plasmon resonance biosensing

Jia Zhang, Ying Sun, Hua Zhang, Bo Xu, Hanqi Zhang, Daqian Song*

College of Chemistry, Jilin University, Qianjin Street 2699, Changchun 130012, PR China

HIGHLIGHTS

- Triangular silver nanoplates were prepared and used to amplify the SPR signal.
- Triangular silver nanoplates are preserved by MPA and chitosan polymer.
- The proposed substrate immobilizes antibodies directly without modification.
- The LOQ of present method for analyte is 32 times lower than that based on Au film.

GRAPHICAL ABSTRACT

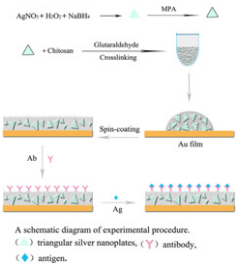

A schematic diagram of experimental procedure. (△) triangular silver nanoplates, (Y) antibody, (◆) antigen.

ARTICLE INFO

Article history:
Received 23 October 2012
Received in revised form
29 December 2012
Accepted 17 January 2013
Available online 25 January 2013

Keywords:
Triangular silver nanoplate
Chitosan
Surface plasmon resonance
Bovine IgG

ABSTRACT

This paper reports the utilization of triangular silver nanoplates (TSNPs) to enhance the sensitivity of surface plasmon resonance (SPR) biosensor. TSNPs modified with 3-mercaptopropinic acid (MPA) were simply mixed with chitosan and glutaraldehyde to form TSNPs/chitosan composite. The composite was deposited on Au film as immobilization substrate for SPR biosensor. The novel structures of TSNPs are preserved against etching by MPA and chitosan polymer. Moreover, chitosan cross-linked by glutaraldehyde enables antibody to be immobilized on fabricated substrate directly via Schiff alkali reaction. In the optimized conditions, the resulting biosensor based on TSNPs/chitosan composite shows a satisfactory response to bovine IgG in the concentration range of 0.075–40.00 μg mL^{-1}. While the biosensor based on chitosan without TSNPs shows a response in the concentration range of 0.6–40 μg mL^{-1} and the biosensor based on Au film shows a response in the concentration range of 2.5–40 μg mL^{-1}. The experiment results show that the sensitivity of SPR biosensor based on TSNPs/chitosan composite was significantly enhanced and the immobilization procedure of antibody was simplified.

1. Introduction

Surface plasmon resonance (SPR) biosensors have become an indispensable tool for studying biomolecular interactions in pharmaceutical and biomedical research over the past decades. One of the main drawbacks that impede further development of SPR applications is the lack of sufficient sensitivity to reliably detect small changes in refractive index caused by compounds in low concentration at the sensing surface [1,2]. Several novel SPR biosensor structures and approaches are reported to address such limitations, such as gold nanoparticles [3,4], magnetic nanoparticles [5,6], carbon nanotubes [7], ZnO–Au nanocomposites [8], and functionalized parylene film [9]. Specifically, plentiful methods have focused on developing substrate based on noble metal nanoparticles such as gold and silver. Systems based on noble metal nanoparticles can be easily prepared and have fairly high enhancement factor because of the strong plasmonic coupling between noble metal nanoparticles and gold or silver substrates, which induces electric field enhancement and leads to high detection sensitivity [10].

* Corresponding author. Tel.: +86 431 85168399.
E-mail address: songdq@jlu.edu.cn (D. Song).

0003-2670/$ – see front matter © 2013 Elsevier B.V. All rights reserved.
http://dx.doi.org/10.1016/j.aca.2013.01.034

Au nanoparticles are often chosen for sensitivity enhancement in biosensing due to its chemical stability and resistance to oxidation, while silver has higher refractive index sensitivity [11,12]. From an optical sensing point of view, the silver particles are more desirable because they provide a stronger and sharper plasmon resonance curve whose peak wavelength can be more accurately determined, especially when valid measures are taken to preserve their excellent properties in practical applications [13]. Moreover, particle shape also plays a large role in determining the sensitivity. Nanoparticles with sharp tips (nanotriangles, bipyramids) exhibit especially high refractive index sensitivities [14,15]. For example, it was determined that triangular silver nanoplates (TSNPs) had a much higher sensitivity (350 nm/RIU) than silver nanospheres (160 nm/RIU), while it is 170 nm/RIU for Au nanorod and 60 nm/RIU for Au nanospheres [16–18]. The anisotropic nature of TSNPs supports large surface charge polarizability and increases local field enhancement which is postulated to lead to high refractive index sensitivities [19]. Three sharp vertices or tips of triangular nanoplates contribute significantly to their optical and electronic properties [20]. These tips act as "hot spots" and are very sensitive to bulk and local dielectric changes. Consequently, triangular nanoplates have one of the highest possible dielectric shifts of existing nanoparticle types [15]. Recently, TSNPs have been successfully used to enhance charge carrier generation in organic photovoltaic films [21]. Silver nanoplate contrast agent for in vivo molecular photoacoustic imaging was reported [22]. DNA-silver nanoplate conjugates were also synthesized for diagnostic application [23]. A thiol-frozen approach was proposed to stabilize high-energy structure of TSNPs. It was found that a small amount of thiol could completely prevent the evolution of nanoplates [24]. The remarkable optical properties enable triangular shaped nanoplates to be attractive candidate for biosensing. However, there have been very few reports exploring triangular structure for the sensitivity enhancement of SPR detection for either nucleic acids or proteins. It is essential to develop strategies to stabilize triangular silver nanostructures while retaining their excellent plasmonic properties for use as effective enhancers in SPR sensing. Therefore, efforts focused on the development of new adhesion layers and sustained silver-based SPR chips are expected [10].

Chitosan is one of the most interesting biopolymer that can be easily handled in biomolecules immobilization due to its great film-forming ability, nontoxicity, mechanical strength, and biocompatibility [25]. Covalent crosslinking for chitosan leads to formation of hydrogels with a permanent network structure, since irreversible chemical links are formed. They exhibit good mechanical properties and can overcome dissolution, even in extreme pH conditions. Therefore, it is a very suitable substrate for immobilizing bioactive molecules and constructing biosensors [26]. In the case of chitosan surfaces, SPR has been utilized to quantify binding of ferric ions [27] and the conjugation of coiled peptides via enzymatic oxidation [28].

In the present work, TSNPs modified with MPA were mixed with chitosan and cross-linked by glutaraldehyde. The performance of SPR biosensor was improved by spin-coating the SPR biochip with TSNPs/chitosan composite. Differing from employing common spherical nanoparticles to improve the performance of SPR biosensor, triangular silver nanostructure was used to induce electromagnetic coupling and amplify the response of the binding of antigen to antibody. Chitosan polymer wrapping TSNPs efficiently protected TSNPs against etching for a robust biosensor. In addition, glutaraldehyde served as cross-linking agent toward chitosan polymer and provided an active substrate interface with sufficient aldehyde groups. Thus antibody could be immobilized directly. The experiment results show that the sensitivity of SPR biosensor based on TSNPs/chitosan composite could be significantly enhanced and the immobilization procedure of antibody was simplified.

2. Materials and methods

2.1. Reagents

Bovine IgG, rabbit anti-bovine IgG and human IgG were purchased from Beijing Boisynthesis Biotechnology Company. Bovine serum albumin (BSA) was purchased from Ding Guo Biotechnology Company (Beijing, China). Polyvinylpyrrolidone (PVP, weight-average molecular weight Mw = 29,000 g mol^{-1}), 3-mercaptopropinic acid (MPA), 1-ethyl-3-(3-dimethylaminopropyl) carbodiimide (EDC) and *N*-hydroxysuccinimide (NHS) were purchased from Jkchemical. Chitosan (molecular weight = 1,000,000; degree of deacetylation ≥95%) was purchased from Aladdin. Silver nitrate, trisodium citrate, hydrogen peroxide, sodium borohydride, sodium hydroxide, acetic acid, ethanol, and all other chemicals were of analytical reagent grade. All the solutions were prepared with ultra pure water, and all the glassware was cleaned with aqua regia before the experiments.

Bovine IgG, rabbit anti-bovine IgG and human IgG were stored at −20 °C and all other biological reagents were stored at 4 °C. Sodium phosphate buffered saline (PBS, 0.01 mol L^{-1}, pH 7.4) was used as running buffer.

2.2. Equipment

The wavelength modulation SPR analyzer installed in our laboratory was used [29]. It is working with Kretschmann configuration to achieve the resonant condition by attenuated total reflection (ATR) in a prism. A 2 nm adhesive layer of Cr followed by a 50 nm layer of Au was deposited on a K9 glass slide, then the glass slide with Au film was put on base of a prism (K9 glass) using a suitable index matching oil. A halogen tungsten lamp is used as the excitation light source. The light passes through a polarizer and two lenses and becomes TM-polarized parallel light. The parallel polychromatic light beam passes through the optical prism and excites surface plasmon at the interface between the Au film and the sample solution. The output light is guided into the optical fiber and then enters the spectrophotometer. A charge-coupled device (CCD) was used as the detector.

2.3. Assay procedure

2.3.1. Synthesis and characterization of triangular silver nanoplates

In a typical experiment, silver nitrate (0.05 mol L^{-1}, 100 μL), trisodium citrate (75 mmol L^{-1}, 1.0 mL), PVP, (17.5 mmol L^{-1}, 0.50 mL) and H_2O_2 (30 wt%, 120 μL) were added in 38 mL aqueous solution and vigorously stirred at room temperature. $NaBH_4$ (100 mmol L^{-1}, 400 μL) was rapidly injected into this mixture to initiate the reduction, immediately leading to a light-yellow solution. After about 25 min, the colloidal solution turned to a deep yellow due to the formation of small silver nanoparticles. Within the next several seconds, the morphology started to change from particles to triangular nanoplates accompanied by the solution color changing rapidly from deep yellow to red, green, and blue. The entire transition from nanoparticles to nanoplates typically took half an hour. The size and shape of TSNPs were tested using transmission electron microscope (TEM). The samples for TEM were obtained by placing drops of each sample on a copper grid. UV–vis absorption spectra of TSNPs was also obtained. After MPA (0.4 mmol L^{-1}, 25 μL, pH 7.0, adjusted by sodium hydroxide solution) was added to prepared TSNPs solution and stirred for 30 min, the TSNPs solution was centrifuged at 14,000 rpm to remove MPA molecules in solution and 2.0 mL water was added to the precipitate. UV–vis absorption spectra of TSNPs modified by MPA were also obtained.

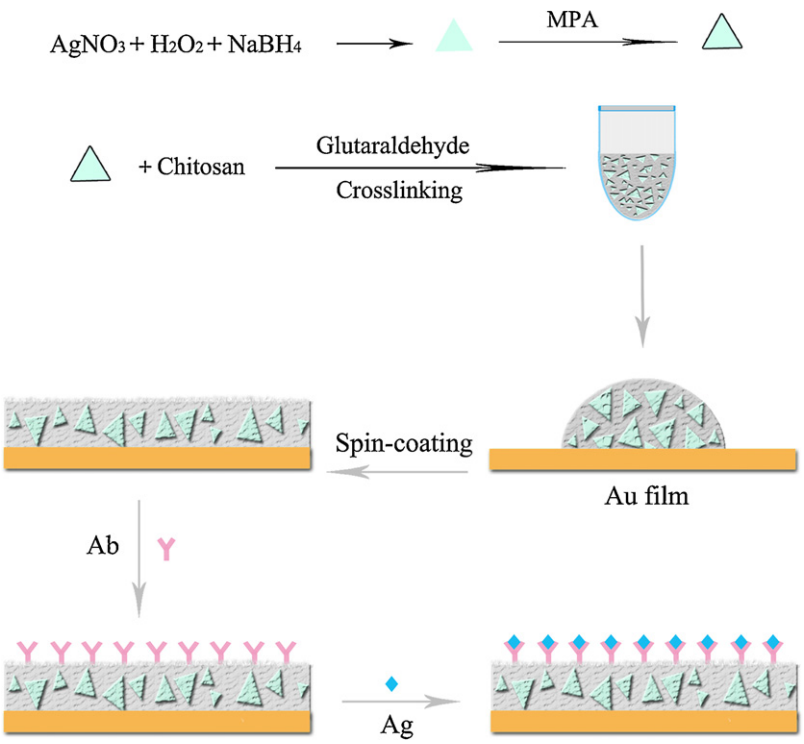

Fig. 1. A schematic diagram of experimental procedure. (▲) TSNPs, (Y) antibody, (◆) antigen.

2.3.2. Preparation of sensing substrate based on TSNPs/chitosan composite

Cross-linking and spin-coating methods were employed to fabricate the substrate. A typical procedure was as follows: 0.4 mL of condensed TSNPs solution was mixed with 1.5 mL of chitosan solution (0.16 wt%, and the concentration of HAc was 35 mmol L^{-1}) and 0.1 mL of glutaraldehyde aqueous solution (1.5 wt%). The resulting solution was mixed completely by a vortex for 30 min. The glass slide with 50 nm layer of Au film was first cleaned with ethanol and deionized water respectively, and then dried with gaseous nitrogen. After 0.2 mL of TSNPs/chitosan composite was deposited on the Au film, the spin-coating was performed in a two-step procedure: (1) 500 rpm for 5 s; (2) 3500 rpm for 30 s. After that, the glass slide was dried in air at room temperature for 24 h to fabricate the substrate based on TSNPs/chitosan composite. The control experiment was made by spin-coating chitosan of identical concentration without TSNPs on the Au film. The prepared glass slide was stored at air temperature prior to be used.

2.3.3. Immobilization of antibody

The sensor substrate fabricated as described above was fixed in the SPR system under a flow cell. Deionized water was first injected into the flow cell. Then PBS was injected into the flow cell as the baseline solution. After the resonant wavelength kept constant, rabbit anti-bovine IgG was injected into the flow cell to covalently attach to the aldehyde-activated surfaces of substrate. After 12 h, PBS buffer was injected into the flow cell to wash off noncovalently bound antibody and to stabilize the baseline. Prior to the analysis, 1 mol L^{-1} ethanolamine hydrochloride (pH 8.0) was used to block the non-specific binding sites on the biosensor surface. A schematic diagram of the experimental procedure is shown in Fig. 1. The same immobilization procedure was applied in the control experiment.

For traditional SPR biosensor substrate, the glass slide was also fixed under the flow cell. After PBS buffer was injected into the flow cell as the baseline solution, 10 mmol L^{-1} MPA was injected into the flow cell and incubated for 3 h. After —COOH group was activated with NHS (30 mg mL^{-1}) under the catalysis of EDC (30 mg mL^{-1}) for 20 min, the rabbit anti-bovine IgG was injected into the flow cell. The following procedures were the same as that mentioned above.

2.3.4. Immunoassay

All SPR experiments were conducted at room temperature. After rabbit anti-bovine IgG was immobilized on the surface of the biosensor, different concentrations of bovine IgG diluted with PBS buffer were separately injected into the flow cell. Free antigens could interact with antibodies immobilized on the biosensor surface and the amount of antigens coupling with the antibodies was monitored as a shift of the resonant wavelength. After 40 min, PBS buffer was injected into the flow cell for 30 min. Due to a large amount of ions in the PBS, the antigen can be dissociated from the antibody immobilized on the surface of the biosensor and removed from the flow cell by impulse injection of the PBS [30]. After the antigen was removed from the flow cell, another sample was introduced into the flow cell. All experiments were conducted in triplicate to examine the reliability of the assays.

To evaluate the selective binding of bovine IgG, human IgG and BSA were determined by the same procedure.

2.3.5. Regeneration

When the immunoassay was finished, the prism was taken away from the flow cell. The glass slide was ultrasonically cleaned separately with ethanol and distilled water, then dried with gaseous nitrogen. The Au film could be used repeatedly.

3. Results and discussion

3.1. Synthesis and characterization of triangular silver nanoplates

In the chemical reduction scheme, silver nanoplates are prepared by reducing $AgNO_3$ with $NaBH_4$ in the presence of trisodium citrate, PVP and H_2O_2 [31]. H_2O_2 plays a critical role for the triangular plate formation. Only quasi-spherical silver nanoparticles can

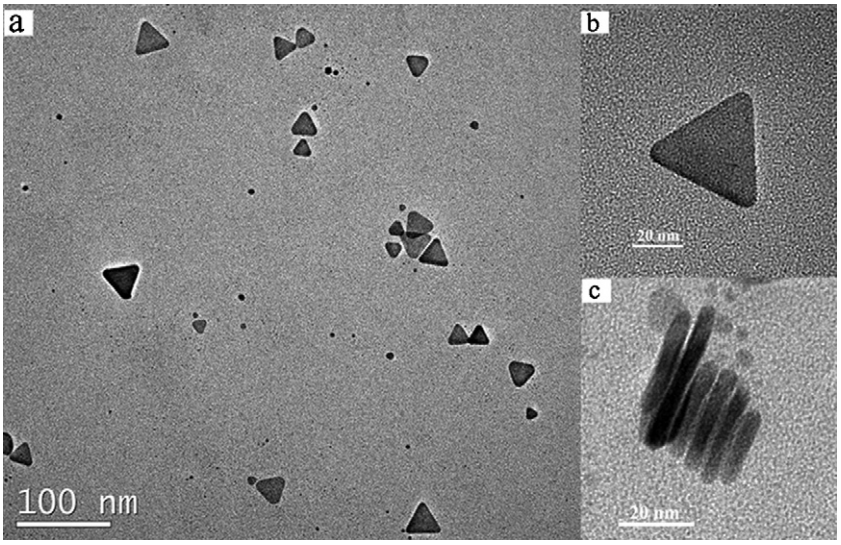

Fig. 2. Transmission electron microscope (TEM) image of TSNPs (a); high resolution TEM image of a typical triangular silver nanoplate (b); and TEM image of TSNPs stacks (c).

be obtained in the absence of H_2O_2. Upon the injection of $NaBH_4$, silver ions are partially reduced to form small silver nanoparticles, which are temporarily stabilized by the adsorption of citrate and borohydride ions. Due to the Ag–citrate coordinating interaction and the presence of the powerful etchant, H_2O_2, the nuclei of silver nanoparticles contain many defects, including the twinned defects that favor the planar growth into plate shapes. Their expansion along the twin plane into high-aspect-ratio nanoplates is enhanced by the fast growth of side facets, typically (1 0 0). The effect of H_2O_2 in this reaction is to promote the nucleation of plates by removing less stable silver nanoparticles of other structures in synergy with citrate ions. In addition, $NaBH_4$ not only functions as a reducing agent but also works as a capping ligand that contributes to the reaction kinetics and morphology control. The advantage of having PVP in the reaction is the improvement of the size distribution of the nanoplates. The size and shape of prepared TSNPs were characterized by TEM. As shown in Fig. 2a, most of the nanoplates formed have well-defined triangular structure and the average edge length of TSNPs is 30 ± 10 nm. Fig. 2b shows high resolution photograph of a typical triangular silver nanoplate. Some silver nanoplates tend to stack upon each other face-to-face and stand vertically on their edges, making it convenient to estimate their thicknesses. Fig. 2c reveals uniform thickness of 6 nm for the formed TSNPs.

Fig. 3a shows UV–vis absorption spectrum of the TSNPs in solution. It is well known that spherical silver nanoparticles show a characteristic peak at about 400 nm. In this paper, TSNPs in solution have three adsorption peaks at 792 (strong), 498 (medium) and 327 nm (weak but sharp) corresponding to in-plane dipole, in-plane quadrupole and out-of-plane quadrupole resonances, respectively. In line with previous studies, the out-of-plane dipole resonance was not resolved in the spectrum because of its weak and broad feature. The quadrupole plasmon modes of the nanoplates are of particular interest, because these modes can only be identified for colloidal dispersions with sufficiently high concentrations of nanoplates that also have relatively narrow particle size and shape distributions (approximately <20%) [20]. The TEM photograph and UV–vis absorption spectrum confirmed that TSNPs were synthesized successfully.

Triangular silver nanoplates exhibit highly tunable architecture-dependent optical properties. However, these structures also have very high surface energies, especially at their tips and edges, where the silver atoms can be readily oxidized. This oxidation may cause truncation of the tips of the plates and force the excellent properties to fade away, which seriously hinder its wide application. A thiol-frozen approach to stabilize high-energy structure of triangular silver nanoplate was proposed by Jiang et al. [24]. It was found that a small amount of thiol could completely prevent the evolution of nanoplates. In previous work, 16-mercaptohexadecanoic acid (MHA) was used as a surface passivating reagent and bound strongly to the silver nanoplate surface presumably via Ag—S bond to prevent their etching for further silica coating of TSNPs [32]. Therefore, MPA was used as protective agent for TSNPs in our experiment for maintaining the novel structure. As shown in Fig. 3b, dipole resonance absorption peak of the TSNPs has a shift of 5 nm after modified with MPA. The UV–vis absorption spectrum of the TSNPs in solution suggests that MPA is adsorbed to the TSNPs surface successfully.

3.2. Preparation of substrate based on TSNPs/chitosan for SPR biosensor

Covalent crosslinking for chitosan leads to formation of hydrogels with a permanent network structure, since irreversible chemical links are formed. They exhibit good mechanical properties and can overcome dissolution, even in extreme pH conditions. Here, chitosan was simply mixed with TSNPs and covalently

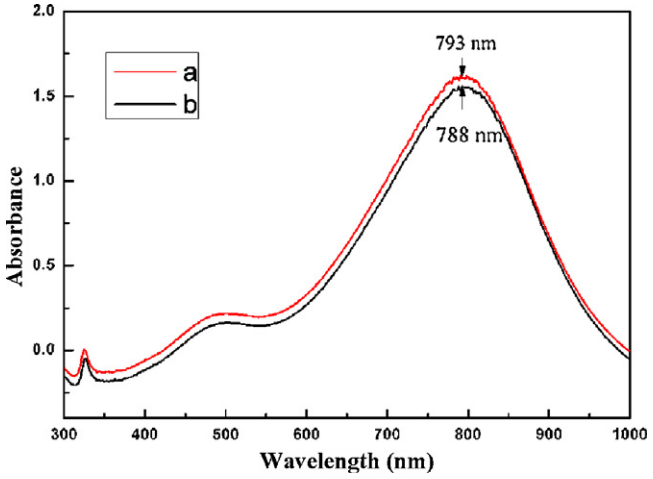

Fig. 3. UV–vis absorption spectra of TSNPs (a) and TSNPs modified by MPA (b).

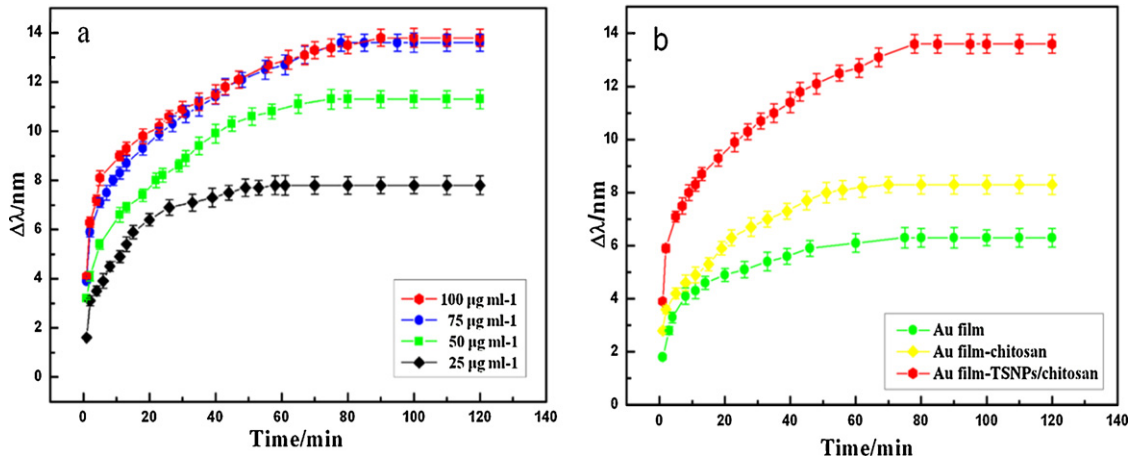

Fig. 4. The kinetic adsorption curves of immobilization of rabbit anti-bovine IgG at different concentrations on fabricated substrate (a) and the kinetic adsorption curves of immobilization of rabbit anti-bovine IgG at the concentration of 75 μg mL^{-1} on different substrates (b).

cross-linked on the surface of Au film by glutaraldehyde. The composite substrate allows adsorption of bioactive compounds without dissolution and displays an active interface with abundant aldehyde groups for immobilization of antibody. Spin-coating technology was employed to form comparatively homogeneous coating on the Au film of the SPR biosensor. Chitosan membrane on the surface of Au film is required to be of appropriate thickness. On one side, Au film and TSNPs must be completely covered with the membrane. On the other side, it has to be thin enough to ensure that SPR resonance signals could be detected. To optimize the chitosan concentration, chitosan solution at different concentrations (0.8, 1.6, and 2.4 mg mL^{-1}) were deposited on SPR interfaces by spin-coating at an acceleration of 500 rpm for 5 s, and then 3500 rpm for 30 s. The thicknesses evaluated by Talystep were about 18 nm for 0.8 mg mL^{-1} and 45 nm for 1.6 mg mL^{-1}. However, relatively homogeneous membrane could not be attained when the concentration of chitosan solution was 2.4 mg mL^{-1}. Taking the average edge length of 30 nm for TSNPs into consideration, chitosan solution of 1.6 mg mL^{-1} was chosen as the suitable concentration for TSNPs to fabricate substrate of SPR biosensor.

When the substrate was used, a red-shift of SPR curves could be observed. The red shift of resonant wavelength was about 42 nm compared with that obtained with bare Au film. The result should be due to the increased substrate thickness and interaction between TSNPs and Au film. Meanwhile, the red shift of resonant wavelength in some wavelength range is beneficial to the sensitivity of wavelength modulation SPR biosensor [33,34].

3.3. Covalent immobilization of rabbit anti-bovine IgG

To examine whether the antibody can be directly immobilized on the active interface of the modified Au film without further chemical treatment, the rabbit anti-bovine IgG at different concentrations was separately injected into the flow cell to perform its binding on the substrate. As expected, the rabbit anti-bovine IgG can be effectively immobilized on the substrate through covalent attachment. Fig. 4a represents the kinetic adsorption curves for immobilization of rabbit anti-bovine IgG. It is noticeable that the resonant wavelength shows an obvious shift at first. Then, with the time increases, the resonant wavelength increases slowly and seems to be unchanged in 80 min, which indicates that the immobilization of antibody on the biosensor surface is completed effectively. With the increase of the concentration of rabbit anti-bovine IgG, more antibodies were immobilized on the biosensor surface, resulting in the resonant wavelength moving to the longer wavelength. When the antibody immobilized on the biosensor surface reached saturation, the resonant wavelength kept a constant value. It can be seen from Fig. 4a that the maximum resonant wavelength shifts for the immobilization of antibody at the concentrations of 75 and 100 μg mL^{-1} are almost the same. As a result, 75 μg mL^{-1} was chosen as the optimum concentration for the detection of bovine IgG. When the concentration of rabbit anti-bovine IgG was 75 μg mL^{-1}, the maximum shift of the resonant wavelength is 13.6 nm within 80 min.

Traditionally, the SPR biosensor surface needs to be activated before immobilization and molecular self-assembly was used to form a sensing layer on the Au film substrate. However, in this sensor, the active interface contains sufficient aldehyde groups and antibody could be immobilized on the substrate directly, which greatly simplify the operation and save the test cost and time.

In order to evaluate the effects of TSNPs on performance improvement for SPR biosensor, the substrate based on chitosan cross-linked by glutaraldehyde without TSNPs and traditional substrate based on Au film were also investigated. Fig. 4b shows the kinetic adsorption curves of 75 μg mL^{-1} rabbit anti-bovine IgG immobilized on the TSNPs/chitosan composite substrate, chitosan substrate and traditional Au film substrate. The maximum shifts of the resonant wavelength are 13.6 nm for substrate based on TSNPs/chitosan composite, 8.3 nm for substrate based on chitosan without TSNPs, and 6.3 nm for substrate based on Au film. Compared with traditional Au film substrate, the chitosan substrate has a relatively rough interface which is beneficial to antibody immobilization. When the TSNPs/chitosan composite was used as substrate, the active interface immobilized more antibodies and the signal for antibody immobilization was significantly amplified. The thickness of the sensing membrane increases and the resonant wavelength moves to longer wavelength, which also lead to the signal amplification of the wavelength-modulation SPR biosensor. The results demonstrate that active interface of the fabricated substrate plays a valuable role for the simple self-immobilization of antibodies and the TSNPs/chitosan composite substrate can be utilized for the development of effective biosensor platforms.

3.4. Determination of bovine IgG

To demonstrate the potential sensitivity of TSNPs/chitosan composite substrate of SPR biosensor, bovine IgG at different concentrations was separately injected into the flow cell at room temperature after the rabbit anti-bovine IgG was immobilized on the surface of the substrate. The shifts of resonant wavelength

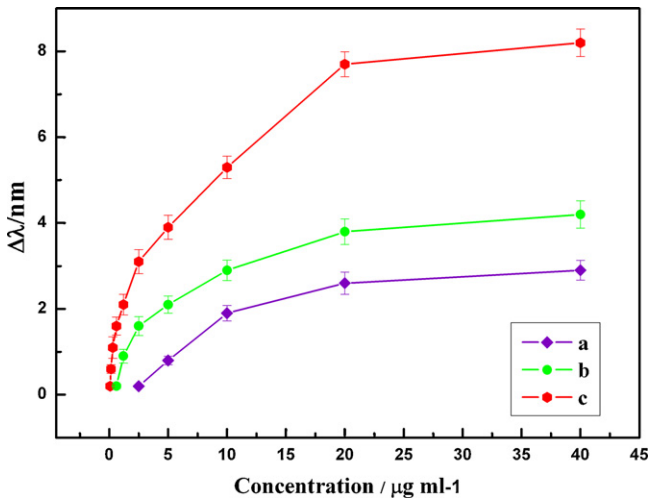

Fig. 5. The relationship between the shifts of the resonant wavelength and different concentrations of bovine IgG: biosensor based on Au film (a); biosensor based on chitosan (b); and biosensor based on TSNPs/chitosan composite (c).

due to antibody–antigen immunoreaction were measured in real time. Fig. 5 shows the relationship between the shifts in the resonant wavelength and the concentrations of bovine IgG. The SPR biosensor based on TSNPs/chitosan composite substrate shows a good response to bovine IgG in the concentration range of 0.075–40.00 μg mL^{-1}. The minimum shift of resonant wavelength is 0.20 nm at 0.075 μg mL^{-1} and the maximum shift is 8.20 nm at 40.00 μg mL^{-1}. The SPR biosensor based on chitosan substrate without TSNPs shows a good response to bovine IgG in the concentration range of 0.60–40.00 μg mL^{-1}. The shift of resonant wavelength is 0.20 nm at 0.60 μg mL^{-1} and 4.20 nm at 40.00 μg mL^{-1}. The SPR biosensor based on Au film substrate shows a response to human IgG in the concentration range 2.50–40.00 μg mL^{-1}. The shift of resonant wavelength is 0.20 nm at 2.50 μg mL^{-1} and 2.90 nm at 40.00 μg mL^{-1}. With the increase of concentration of bovine IgG, the binding sites of the antibodies immobilized on the surface will be saturated. When the concentration of the bovine IgG was higher than 40 μg mL^{-1}, no further obvious shift of the resonant wavelength was observed and this concentration is the upper determination limit. The limit of quantification (LOQ) is the lowest concentration of an analyte that can be quantitatively determined by the present method. The LOQ by the biosensor based on TSNPs/chitosan composite substrate is about 8 times lower than that based on chitosan substrate without TSNPs and 32 times lower than that obtained by the sensor based on Au film.

The key to a wider application of SPR biosensors is the development of an efficient SPR substrate that not only can provide strong enhancement factors, but also can be stable, reproducible, inexpensive and easy to fabricate and handle. In this paper, triangular silver nanostructure was used to induce electromagnetic coupling and amplify the response of the binding of antigen to antibody. Triangular nanoplates exhibit especially high sensitivity to the refractive index change of the surrounding medium as well as strong electromagnetic-field enhancement due to their unique anisotropic nature. Because of the location of electromagnetic hot spots near the tips and edges of the nanoplates, they have one of the highest possible dielectric shifts of existing nanoparticle types [15]. It is evident from the above experiment data that most of the enhancement effects owe to the influence of TSNPs of the fabricated substrate. The electronic coupling between the TSNPs and the surface plasmon wave leads to the amplification of the SPR response originating from the dielectric changes of the substrate upon binding of the antigen–antibody complexes. In addition, the thickness of the sensing membrane increases and the resonant wavelength moves to longer wavelength, which also lead to the sensitivity enhancement of the wavelength-modulation SPR biosensor. The immunoassay results demonstrate that the fabricated substrate containing TSNPs could effectively enhance the SPR signal in biomolecular interactions.

As can be seen in Fig. 5, the shift of the resonant wavelength does not linearly increase with the increase of the concentration of bovine IgG in certain concentration range. The reaction of antigen (Ag) and antibody (Ab) can be expressed as follows: Ag + Ab = AgAb, the binding constant is K_A.

$$K_A = \frac{[AgAb]}{[Ag][Ab]} \quad (1)$$

where [AgAb] is corresponding to the SPR biosensor signal $\Delta\lambda_{eq}$, [Ag] is the concentration of antigen in the solution, [Ab] is corresponding to $(\Delta\lambda_{max} - \Delta\lambda_{eq})$. $\Delta\lambda_{eq}$ is the biosensor response at equilibrium. $\Delta\lambda_{max}$ is the SPR response corresponding to the maximum capacity of binding antigen on the sensor surface. So Eq. (1) can be expressed as

$$\frac{\Delta\lambda_{eq}}{[Ag]} = K_A\Delta\lambda_{max} - K_A\Delta\lambda_{eq} \quad (2)$$

$\Delta\lambda_{eq}$ increases with the increase of concentration of antigen ([Ag]) in the solution. It is seen from the Eq. (2) that the $\Delta\lambda_{eq}$/[Ag]

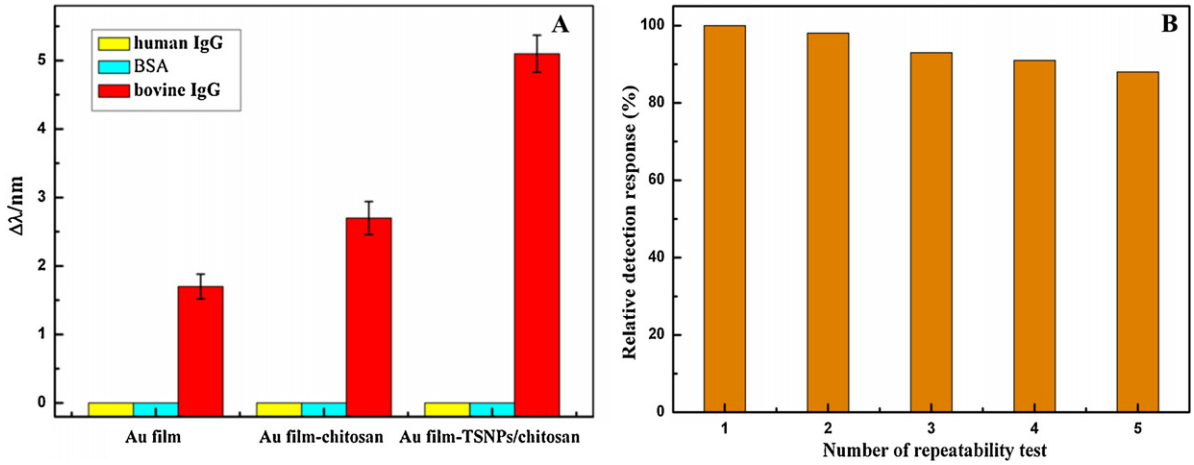

Fig. 6. The shift of resonant wavelength measured by SPR biosensor for different antigens (bovine IgG, BSA and human IgG) in different assays (A); the repeatability test of SPR Au film and relative detection response (B).

decreases with the increase of $\Delta\lambda_{eq}$. So the slope of the relationship curve between the shift of the resonant wavelength and the concentration of bovine IgG decreases with the increase of the concentration of antigen, which is in accordance with the experimental results.

The specificity is also demonstrated by detecting human IgG and BSA under the same conditions. After the rabbit anti-bovine IgG was immobilized on the surface of the biosensor, human IgG and BSA at the concentrations of 10 $\mu g\,mL^{-1}$ were separately injected into the flow cell for 45 min. There are no observable shifts of the resonant wavelength (Fig. 6A), which indicates the selective binding of bovine IgG.

3.5. Regeneration

When a series of antibody–antigen binding assays were performed, the regeneration of biosensor was needed. The prism was taken away and the glass slide was ultrasonically cleaned with ethanol and distilled water respectively, then dried with gaseous nitrogen. After the TSNPs/chitosan composite was deposited on the Au film by spin-coating, the modified Au film could be applied to antibody immobilization for the next measurement. The same Au film can be used to prepare the sensing substrate for about five times. The sensor surface stabilized around 88% initial activities after regeneration for the fifth time (Fig. 6B).

4. Conclusions

In this study, a new strategy for effective immobilization of antibody and sensitivity enhancement in the development of SPR biosensor is presented. The TSNPs/chitosan composite was prepared and used as substrate by spin-coating. Antibodies were immobilized on the fabricated substrate directly without further chemical modification. The limit of quantification for bovine IgG based on TSNPs/chitosan composite is 0.075 $\mu g\,mL^{-1}$ and the resulting biosensor shows a satisfactory response to bovine IgG in the concentration range of 0.075–40.00 $\mu g\,mL^{-1}$. The performance of the biosensor is attributed to high sensitivity of TSNPs to the refractive index changes and good biocompatibility of chitosan. Meanwhile, this SPR biosensor can provide a sensitive biosensing system and serve as a good alternative detection technique to the conventional SPR biosensor.

Acknowledgements

This work was supported by National Natural Science Foundation of China (Nos. 20727003, 21075049, 21105037), Program for New Century Excellent Talents in University (No. NECT-10-0443), Special-funded Programme on National Key Scientific Instruments and Equipment Development (No. 2012YQ090194) and Science and Technology Developing Foundation of Jilin Province (Nos. 20100356, 20110162).

References

[1] J. Wang, Small 1 (2005) 1036–1043.
[2] C.F. Gao, Z.D. Lu, Y. Liu, Q. Zhang, M.F. Chi, Q. Cheng, Y.D. Yin, Angew. Chem. Int. Ed. 51 (2012) 5629–5633.
[3] L.A. Lyon, M.D. Musick, M.J. Natan, Anal. Chem. 70 (1998) 5177–5183.
[4] M. Riskin, Y.B. Amram, R.T. Vered, V. Chegel, J. Almog, I. Willner, Anal. Chem. 83 (2011) 3082–3088.
[5] Y. Sun, Y.P. Bai, D.Q. Song, X.Z. Li, L.Y. Wang, H.Q. Zhang, Biosens. Bioelectron. 23 (2007) 473–478.
[6] Y. Sun, D.Q. Song, Y.P. Bai, L.Y. Wang, Y. Tian, H.Q. Zhang, Anal. Chim. Acta 624 (2008) 294–300.
[7] W.H. Hu, Z.S. Lu, Y.S. Liu, C.M. Li, Langmuir 26 (2010) 8386–8391.
[8] L.Y. Wang, J. Wang, S.L. Zhang, Y. Sun, X.N. Zhu, Y.B. Cao, X.H. Wang, H.Q. Zhang, D.Q. Song, Anal. Chim. Acta 653 (2009) 109–115.
[9] B.J. Jeona, M.H. Kim, J.C. Pyuna, Sens. Actuat. B 154 (2011) 89–95.
[10] A. Abbas, M.J. Linman, Q. Cheng, Biosens. Bioelectron. 26 (2011) 1815–1824.
[11] M. Wang, C. Sun, L. Wang, X. Ji, Y. Bai, T. Li, J.H. Li, J. Pharm. Biomed. Anal. 33 (2003) 1117–1125.
[12] Z.P. Wang, J.Q. Hu, Y. Jin, X. Yao, J.H. Li, Clin. Chem. 52 (2006) 1958–1961.
[13] K.M. Mayer, J.H. Hafner, Chem. Rev. 111 (2011) 3828–3857.
[14] J. Burgin, M.Z. Liu, P. Guyot-Sionnest, J. Phys. Chem. C 112 (2008) 19279–19282.
[15] M.J. Banholzer, N. Harris, J.E. Millstone, G.C. Schatz, C.A. Mirkin, J. Phys. Chem. C 114 (2010) 7521–7526.
[16] J.J. Mock, D.R. Smith, S. Schultz, Nano Lett. 3 (2003) 485–491.
[17] S. Underwood, P. Mulvaney, Langmuir 10 (1994) 3427–3430.
[18] K.M. Mayer, S. Lee, H. Liao, B.C. Rostro, A. Fuentes, P.T. Scully, C.L. Nehl, J.H. Hafner, ACS Nano 2 (2008) 687–692.
[19] D.E. Charles, M. Gara, D. Aherne, D.M. Ledwith, J.M. Kelly, W.J. Blau, Plasmonics 6 (2011) 351–362.
[20] J.E. Millstone, S.J. Hurst, G.S. Métraux, J.I. Cutler, C.A. Mirkin, Small 5 (2009) 646–664.
[21] A.P. Kulkarni, K.M. Noone, K. Munechika, S.R. Guyer, D.S. Ginger, Nano Lett. 10 (2010) 1501–1505.
[22] K.A. Homan, M. Souza, R. Truby, G.P. Luke, C. Green, E. Vreeland, S. Emelianov, ACS Nano 6 (2012) 641–650.
[23] J.Y. Kim, J.S. lee, Chem. Mater. 22 (2010) 6684–6691.
[24] X.C. Jiang, Q.H. Zeng, A.B. Yu, Langmuir 23 (2007) 2218–2223.
[25] J. Berger, M. Reist, J.M. Mayer, O. Felt, N.A. Peppas, R. Gurnyb, Eur. J. Pharm. Biopharm. 57 (2004) 19–34.
[26] W.T. Shi, Z.F. Ma, Biosens. Bioelectron. 26 (2010) 1098–1103.
[27] H.A. McIlwee, C.L. Schauer, V.G. Praig, R. Boukherroub, S. Szunerits, Analyst 5 (2008) 673–677.
[28] A. Demolliens, C. Boucher, Y. Durocher, M. Jolicoeur, M.D. Buschmann, G. De Crescenzo, Bioconjugate Chem. 9 (2008) 1849–1854.
[29] J. Wang, L.Y. Wang, Y. Sun, X.N. Zhu, Y.B. Cao, X.H. Wang, H.Q. Zhang, D.Q. Song, Colloids Surf. B: Biointer. 75 (2010) 520–525.
[30] R. Pei, X. Cui, X.E. Yang, Talanta 53 (2000) 481–488.
[31] Q. Zhang, N. Li, J. Goebl, Z.D. Lu, Y.D. Yin, J. Am. Chem. Soc. 133 (2011) 18931–18939.
[32] C. Xue, X.D. Chen, S.J. Hurst, C.A. Mirkin, Adv. Mater. 19 (2007) 4071–4074.
[33] J. Homola, Sens. Actuat. B 41 (1997) 207–211.
[34] J. Homola, I. Koudela, S.S. Yee, Sens. Actuat. B 54 (1999) 16–24.